The Journal of the Astronautical Sciences, Vol. 56, No. 2, April–June 2008, pp. 251–268

# Adaptive Spacecraft Attitude Tracking Control with Actuator Uncertainties[1]

**Hyungjoo Yoon[2] and Panagiotis Tsiotras[3]**

**Abstract**

An adaptive control algorithm for the spacecraft attitude tracking problem when the spin axis directions and/or the gains of the flywheel actuators are uncertain is developed. A smooth projection algorithm is applied to keep the parameter estimates inside a singularity-free region and avoid parameter bursting. Numerical examples show that the controller successfully deals with unknown misalignments of the axis directions as well as the unknown gains of the flywheel actuators.

## Introduction

Adaptive attitude control of spacecraft with uncertain parameters has been studied intensively in the past decade [1–8]. However, most (if not all) of the previous research deals only with uncertainties in the inertia matrix of the spacecraft, assuming that an exact model of the actuators is available. The only exemption the authors are aware of seems to be reference [9], in which disturbances caused by defects of flywheels are estimated and compensated using recursive filtering. However, the control law presented in that work can be applied only for the special case when the reference attitude is the local-vertical-local-horizonal frame for a circular orbit. Subsequently, most results in the literature hinge on the assumption that the torque axis directions and/or input scalings of the actuators (e.g., gas jets, reaction wheels, or CMGs/VSCMGs etc.) are exactly known. This assumption is rarely satisfied in practice because of misalignment of the actuators during installation, aging and wearing out of the mechanical and electrical parts, etc. For most cases the effect of these uncertainties on the overall system performance is not significant. However, for the case of flywheels used as "mechanical batteries" in an Integrated Power and Attitude Control System (IPACS) [8, 10, 11], even small misalignments of the flywheel axes can be detrimental. Flywheels for IPACS applications spin at very high speeds and subsequently have large amounts of stored kinetic energy

[1]Presented as paper AIAA-2005-6392 at the 2005 AIAA Guidance, Navigation, and Control Conference.
[2]NRC Research Associate, Naval Postgraduate School, Monterey, CA 93943. E-mail: hyoon@nps.edu.
[3]Professor, School of Aerospace Engineering. E-mail: tsiotras@gatech.edu.

(and hence angular momentum). Precise attitude control requires proper momentum management, while minimizing spurious output torques. This can be achieved with the use (in the simplest scenario) of at least four flywheels, whose angular momenta have to be canceled or regulated with high precision. If the exact direction of the axes (hence also the direction of the angular momenta) are not known with sufficient accuracy, large output torque errors will impact the attitude of the spacecraft. Similarly, accurate information of the actuator gains are necessary for exact cancelation of the angular momenta. In this article, an adaptive control law is designed for spacecraft attitude tracking using Variable Speed Control Moment Gyros (VSCMGs) [8, 11, 12], whose moments of inertia and gimbal axes directions are not exactly known.

A VSCMG is a spacecraft attitude actuator, which has been recently introduced as an alternative to conventional control moment gyros (CMGs) and reaction wheels (RWs). A conventional CMG has a regulator to keep its flywheel spinning at a constant rate, whereas a VSCMG—as its name implies—is essentially a single-gimbal control moment gyro (CMG), with the flywheel allowed to have variable speed. The VSCMGs are especially suitable for IPACS applications [8], because the variable speed of the flywheels can be used to store/release mechanical (i.e., kinetic) energy at will, while gimbal angle changes can be used to generate the necessary torques for attitude control in an efficient manner owing to the torque amplification effect. The VSCMGs are also suitable for developing and implementing singularity-free steering laws in lieu of standard CMGs, thanks to their additional degrees of freedom [11, 12].

One of the difficulties encountered when designing adaptive controllers dealing with actuator uncertainties for the spacecraft attitude tracking problem is the Multi-Input/Multi-Output (MIMO) form of the equations of motion. The controller has to track at least the three attitude states for full three-axis attitude control. Complete control requires, in general, three or more actuator torques. Much research has been devoted to the adaptive attitude tracking problem. Most previous results in this area have dealt only with the Single-Input/Single-Output (SISO) or the uncoupled Multi-Input case. Slotine et al [1, 13]. proposed adaptive controllers for MIMO systems, but these systems must be Hamiltonian. Furthermore, the uncertainties should appear in the inertia of the spacecraft and/or the Coriolis/centrifugal terms, but not in the actuators. Ge [14] derived an adaptive control law for multi-link robot manipulators with uncertainties in the control input term, but the uncertainty must be in the input scalings and the uncertainty matrix must be diagonal when represented in multiplicative form.

Recently, Chang [15] provided an adaptive, robust tracking control algorithm for nonlinear MIMO systems. His work is based on the "smooth projection algorithm," which has also been used in references [16] and [17] for adaptive control of SISO systems. This algorithm plays a key role in our developments by keeping the parameter estimates inside a properly defined convex set, so that the estimates neither drift into a region where the control law may become singular nor diverge to very large values.

## Problem Statement

Consider a spacecraft with a VSCMG cluster of $N$ flywheels, as shown in Fig. 1. The definition of the axes in Figure 1 is as follows ($i = 1, \ldots, N$):

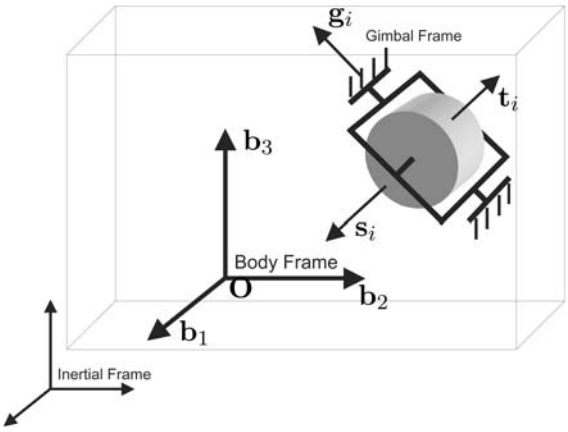


**FIG. 1.** Spacecraft Body with the $i$th VSCMG.

- $\mathbf{g}_i$ : VSCMG gimbal axis unit vector
- $\mathbf{s}_i$ : VSCMG spin axis unit vector
- $\mathbf{t}_i$ : VSCMG transverse axis unit vector (torque vector) given as $\mathbf{t}_i = \mathbf{g}_i \times \mathbf{s}_i$.

The equations of motion of a spacecraft with a cluster of VSCMGs are rather complicated [8, 11, 18]. Thus, in this paper a set of simplified (but still nonlinear) equations will be used to assist with the control law design. The final controller will nonetheless be validated against the complete, nonlinear model in the numerical simulations later on. With a slight abuse of notation, in the sequel we will use boldface symbols to denote both a vector and its representation in the standard basis. This simplification should not cause any problems, as the meaning of the expression (and the corresponding basis used) should be clear from the context. If the need arises to refer to a representation with respect to a specific frame, we will use subscripts to denote the frame used.

The dynamic equations of motion of the spacecraft can be written as [8, 19]

$$\dot{J}\boldsymbol{\omega} + J\dot{\boldsymbol{\omega}} + A_{\mathrm{g}} I_{\mathrm{cg}} \ddot{\boldsymbol{\gamma}} + A_{\mathrm{t}} I_{\mathrm{ws}} \boldsymbol{\Omega}^d \dot{\boldsymbol{\gamma}} + A_{\mathrm{s}} I_{\mathrm{ws}} \dot{\boldsymbol{\Omega}} + \boldsymbol{\omega}^{\times} \mathbf{h} = 0 \tag{1a}$$

$$\mathbf{h} = J\boldsymbol{\omega} + A_{\mathrm{g}} I_{\mathrm{cg}} \dot{\boldsymbol{\gamma}} + A_{\mathrm{s}} I_{\mathrm{ws}} \boldsymbol{\Omega} \tag{1b}$$

where $J = {}^{B}I + A_{\mathrm{s}} I_{\mathrm{cs}} A_{\mathrm{s}}^{\mathrm{T}} + A_{\mathrm{t}} I_{\mathrm{ct}} A_{\mathrm{t}}^{\mathrm{T}} + A_{\mathrm{g}} I_{\mathrm{cg}} A_{\mathrm{g}}^{\mathrm{T}}$ is the total moment of inertia of the spacecraft, ${}^{B}I$ is the combined matrix of inertia of the spacecraft platform and the point-masses of the VSCMGs, $\boldsymbol{\omega}$ is the body rate vector of the spacecraft, and $\boldsymbol{\gamma} = (\gamma_1, \ldots, \gamma_N)^{\mathrm{T}} \in \mathbb{R}^N$ and $\boldsymbol{\Omega} = (\Omega_1, \ldots, \Omega_N)^{\mathrm{T}} \in \mathbb{R}^N$ are column vectors, whose elements are the gimbal angles and the wheel speeds of the VSCMGs with respect to the gimbals, respectively. The matrices $A_* \in \mathbb{R}^{3\times N}$ have as columns the gimbal, spin and transverse directional unit vectors expressed in the body-frame, where $* = \mathrm{g}, \mathrm{s}, \mathrm{t}$. These depend on the gimbal angles as

$$A_{\mathrm{g}} = A_{\mathrm{g0}} \tag{2}$$

$$A_{\mathrm{s}} = A_{\mathrm{s0}}[\cos\boldsymbol{\gamma}]^d + A_{\mathrm{t0}}[\sin\boldsymbol{\gamma}]^d \tag{3}$$

$$A_{\mathrm{t}} = A_{\mathrm{t0}}[\cos\boldsymbol{\gamma}]^d + A_{\mathrm{s0}}[\sin\boldsymbol{\gamma}]^d \tag{4}$$

where the $A_{*0}$'s denote the values of $A_*$ at $\gamma_i = 0$. The symbol $\boldsymbol{x}^d$ denotes the diagonal matrix with elements the components of the vector $\boldsymbol{x}$, and

$\cos \boldsymbol{\gamma} \triangleq [\cos \gamma_1, \ldots, \cos \gamma_N]^{\mathrm{T}}$ and $\sin \boldsymbol{\gamma} \triangleq [\sin \gamma_1, \ldots, \sin \gamma_N]^{\mathrm{T}}$. The matrices $I_{\mathrm{c}^*}$ and $I_{\mathrm{w}^*}$ are diagonal, with elements the values of the inertias of the VSCMG gimbal structure plus flywheel and flywheel-only, respectively. The skew-symmetric matrix $\boldsymbol{\nu}^{\times}$, for $\boldsymbol{\nu} \in \mathbb{R}$,[3] represents the cross product operation. See reference [19] for the details in deriving equation (1).

In general, the total moment of inertia of the spacecraft will change as the VSCMGs rotate about their gimbal axes, so the matrix $J$ is a function of a gimbal angle vector $\boldsymbol{\gamma}$, that is, $J = J(\boldsymbol{\gamma})$. However, this dependence of $J$ on $\boldsymbol{\gamma}$ is weak, especially when the size of the spacecraft main body is large compared to the flywheels. We will therefore assume that $J$ is constant ($\dot{J} = 0$) during controller design. In addition, and in order to simplify the analysis, we will assume that the gimbal acceleration term $A_{\mathrm{g}} I_{\mathrm{cg}} \ddot{\boldsymbol{\gamma}}$ can be ignored. This essentially amounts to gimbal angle rate servo control. It will also be assumed that the gimbal angle rate term $A_{\mathrm{g}} I_{\mathrm{cg}} \dot{\boldsymbol{\gamma}}$ does not contribute significantly to the total angular momentum $\mathbf{h}$ of the spacecraft. These assumptions are standard in the literature [12, 20, 21] and are validated in the Numerical Examples section at the end of the paper.

Under the previous assumptions, one obtains the simplified equations of motion as

$$J\dot{\boldsymbol{\omega}} + C(\boldsymbol{\gamma}, \boldsymbol{\Omega})\dot{\boldsymbol{\gamma}} + D(\boldsymbol{\gamma})\dot{\boldsymbol{\Omega}} + \boldsymbol{\omega}^{\times}\mathbf{h} = 0 \tag{5}$$

where

$$\mathbf{h} \triangleq J\boldsymbol{\omega} + A_{\mathrm{s}} I_{\mathrm{ws}} \boldsymbol{\Omega} \tag{6}$$

and where

$$C(\boldsymbol{\gamma}, \boldsymbol{\Omega}) \triangleq A_{\mathrm{t}} I_{\mathrm{ws}} \boldsymbol{\Omega}^{d}, \quad D(\boldsymbol{\gamma}) \triangleq A_{\mathrm{s}} I_{\mathrm{ws}} \tag{7}$$

Notice that this equation has been derived for a spacecraft with a VSCMG cluster, and therefore it subsumes the reaction wheel case (obtained by setting $\boldsymbol{\gamma}$ to be constant in the above equations), and the conventional CMG case (obtained by setting $\boldsymbol{\Omega}$ to be constant).

The Modified Rodrigues parameters [22–24] (MRPs) are chosen to describe the attitude kinematics of the spacecraft.[4] The MRPs are defined in terms of the Euler principal unit vector $\hat{\boldsymbol{\eta}}$ and angle $\phi$ by $\boldsymbol{\sigma} = \hat{\boldsymbol{\eta}} \tan(\phi/4)$. The MRPs have the advantage of being a minimal parameterization of the attitude (no constraint) while at the same time being well defined for the whole range of rotations [22, 23, 25], i.e., $\phi \in [0, 2\pi)$. The differential equation that governs the kinematics in terms of the MRPs is given by [24, 25]

$$\dot{\boldsymbol{\sigma}} = G(\boldsymbol{\sigma})\boldsymbol{\omega} \tag{8}$$

where

$$G(\boldsymbol{\sigma}) = \frac{1}{2}\left( I + [\boldsymbol{\sigma}^{\times}] + \boldsymbol{\sigma}\boldsymbol{\sigma}^{\mathrm{T}} - \left[ \frac{1}{2}(1 + \boldsymbol{\sigma}^{\mathrm{T}}\boldsymbol{\sigma}) \right] I \right) \tag{9}$$

and $I$ denotes the identity matrix.

Next, we combine the kinetic equation (5) and the kinematic equation (8) into one second-order system. From equation (8), one obtains $\boldsymbol{\omega} = G^{-1}(\boldsymbol{\sigma})\dot{\boldsymbol{\sigma}}$ and

[4]We hasten to point out that the use of the MRPs to describe the kinematics is done without loss of generality. Any other suitable kinematic description could have been used with the conclusions of the paper remaining essentially the same.

$\ddot{\boldsymbol{\sigma}} = G(\boldsymbol{\sigma})\dot{\boldsymbol{\omega}} + \dot{G}(\boldsymbol{\sigma}, \dot{\boldsymbol{\sigma}})\boldsymbol{\omega}$. The total angular momentum, $\mathbf{h}$, written in the body frame can be expressed as $\mathbf{h} = R_I^{\mathcal{B}}(\boldsymbol{\sigma})\mathbf{H}_I$, where $R_I^{\mathcal{B}}(\boldsymbol{\sigma})$ is the rotational matrix from the inertial frame $\mathcal{I}$ to the body frame $\mathcal{B}$, and $\mathbf{H}_I$ is the total angular momentum written in the $\mathcal{I}$-frame. If we assume that no external control/disturbance torques act on the spacecraft, then the total angular momentum of the spacecraft-VSCMG system is conserved (in both magnitude and direction) during a maneuver, and thus $\mathbf{H}_I$ is constant. From equation (5) one can then write

$$G^{-\mathrm{T}}JG^{-1}\ddot{\boldsymbol{\sigma}} - G^{-\mathrm{T}}JG^{-1}\dot{G}G^{-1}\dot{\boldsymbol{\sigma}} + G^{-\mathrm{T}}\boldsymbol{\omega}^{\times}(R_I^{\mathcal{B}}(\boldsymbol{\sigma})\mathbf{H}_I) + G^{-\mathrm{T}}(C\dot{\boldsymbol{\gamma}} + D\dot{\boldsymbol{\Omega}}) = 0 \quad (10)$$

equivalently,

$$\ddot{\boldsymbol{\sigma}} = F^{*}(\boldsymbol{\sigma}, \dot{\boldsymbol{\sigma}}) + G^{*}(\boldsymbol{\sigma}, \boldsymbol{\gamma}, \boldsymbol{\Omega})\boldsymbol{u} \quad (11)$$

where

$$F^{*}(\boldsymbol{\sigma}, \dot{\boldsymbol{\sigma}}) \triangleq H^{*-1}(G^{-\mathrm{T}}JG^{-1}\dot{G}G^{-1}\dot{\boldsymbol{\sigma}} - G^{-\mathrm{T}}\boldsymbol{\omega}^{\times}(R_I^{\mathcal{B}}(\boldsymbol{\sigma})\mathbf{H}_I)) \quad (12a)$$

$$G^{*}(\boldsymbol{\sigma}, \boldsymbol{\gamma}, \boldsymbol{\Omega}) \triangleq -H^{*-1}G^{-\mathrm{T}}Q = -GJ^{-1}Q \quad (12b)$$

$$H^{*}(\boldsymbol{\sigma}) \triangleq G^{-\mathrm{T}}JG^{-1} \quad (12c)$$

$$Q(\boldsymbol{\gamma}, \boldsymbol{\Omega}) \triangleq [C(\boldsymbol{\gamma}, \boldsymbol{\Omega}), D(\boldsymbol{\gamma})] \quad (12d)$$

with control input vector

$$\boldsymbol{u} \triangleq [\dot{\boldsymbol{\gamma}}^{\mathrm{T}}, \dot{\boldsymbol{\Omega}}^{\mathrm{T}}]^{\mathrm{T}} \in \mathbb{R}^{2N\times 1} \quad (13)$$

The second-order equation of motion (11) can be written in state-space form as

$$\frac{\mathrm{d}}{\mathrm{d}t}\begin{bmatrix}\boldsymbol{\sigma}\\ \dot{\boldsymbol{\sigma}}\end{bmatrix} = \begin{bmatrix}0 & I\\ 0 & 0\end{bmatrix}\begin{bmatrix}\boldsymbol{\sigma}\\ \dot{\boldsymbol{\sigma}}\end{bmatrix} + \begin{bmatrix}0\\ I\end{bmatrix}(F^{*}(\boldsymbol{\sigma}, \dot{\boldsymbol{\sigma}}) + G^{*}(\boldsymbol{\sigma}, \boldsymbol{\gamma}, \boldsymbol{\Omega})\boldsymbol{u}) \quad (14)$$

Suppose now that there are uncertainties in the modeling of the actuators, so that the exact values of the initial axis directions at $\boldsymbol{\gamma} = \mathbf{0}$ and scaling input gains are unknown. Let us assume that the actual initial axis direction matrices of the wheels can be expressed as

$$A_{\mathrm{s}0} = A_{\mathrm{s}0}^{\mathrm{n}} + A_{\mathrm{s}0}^{\Delta}, \quad A_{\mathrm{t}0} = A_{\mathrm{t}0}^{\mathrm{n}} + A_{\mathrm{t}0}^{\Delta} \quad (15)$$

where $A_{*0}^{\mathrm{n}}$ are nominal values and $A_{*0}^{\Delta}$ are unknown constant values of the matrices $A_{\mathrm{s}0}$ and $A_{\mathrm{t}0}$. The exact value of the moment of inertia $I_{\mathrm{ws},i}$ of the flywheel of the $i$th VSCMG along the spin axis acts as an input scaling gain (which is a product of the moment inertia and electric/mechanical gains) and is assumed to be unknown for all $i = 1, \ldots, N$, while its nominal value is $I_{\mathrm{ws},i}^{\mathrm{n}}$ and is assumed to be known.

Since we do not know the exact angular momentum of the VSCMG cluster due to the uncertainties in the spin axes directions and the rotational inertia of the flywheels, the total angular momentum $\mathbf{H}_I$ can be expressed as

$$\mathbf{H}_I = \mathbf{H}_I^{\mathrm{n}} + \mathbf{H}_I^{\Delta} \quad (16)$$

where $\mathbf{H}_I^{\mathrm{n}}$ is the known nominal value of $\mathbf{H}_I$ in the inertial frame, and $\mathbf{H}_I^{\Delta}$ is an unknown (in magnitude and direction) constant vector. In addition, the Jacobian matrix $Q$ defined in equation (12d) is also unknown because the exact axes directions are unknown, so $Q^{\mathrm{n}}$ and $Q^{\Delta}$ are defined as the nominal and the uncertain errors of the matrix $Q$, respectively. That is,

$$Q = Q^{\mathrm{n}} + Q^{\Delta} \quad (17)$$

The moment of inertia of the whole spacecraft system $J$ may also be uncertain due to the uncertainties of the axes and inertia of the flywheels, but its effect is small so it is ignored in the sequel.

Dropping the arguments for convenience, the system matrices in (12a) and (12b) can be decomposed as

$$F^* = F^{*\mathrm{n}} + F^{*\Delta}, \quad G^* = G^{*\mathrm{n}} + G^{*\Delta} \tag{18}$$

where,

$$F^{*\mathrm{n}}(\boldsymbol{\sigma}, \dot{\boldsymbol{\sigma}}) \triangleq H^{*-1}(G^{-\mathrm{T}}JG^{-1}\dot{G}G^{-1}\dot{\boldsymbol{\sigma}} - G^{-\mathrm{T}}\boldsymbol{\omega}^{\times}(R_I^{\mathcal{B}}(\boldsymbol{\sigma})\mathbf{H}_I^{\mathrm{n}})) \tag{19a}$$

$$F^{*\Delta}(\boldsymbol{\sigma}, \dot{\boldsymbol{\sigma}}) \triangleq -H^{*-1}(G^{-\mathrm{T}}\boldsymbol{\omega}^{\times}(R_I^{\mathcal{B}}(\boldsymbol{\sigma})\mathbf{H}_I^{\Delta})) \tag{19b}$$

and

$$G^{*\mathrm{n}}(\boldsymbol{\sigma}, \boldsymbol{\gamma}, \boldsymbol{\Omega}) \triangleq -H^{*-1}G^{-\mathrm{T}}Q^{\mathrm{n}} \tag{20a}$$

$$G^{*\Delta}(\boldsymbol{\sigma}, \boldsymbol{\gamma}, \boldsymbol{\Omega}) \triangleq -H^{*-1}G^{-\mathrm{T}}Q^{\Delta} \tag{20b}$$

Notice that $F^{*\Delta}$ is linear in the uncertain elements of the vector $\mathbf{H}_I^{\Delta}$, thus it can be written as

$$F^{*\Delta} = Y_F\Theta_F \tag{21}$$

where $\Theta_F \triangleq \mathbf{H}_I^{\Delta} \in \mathbb{R}^{3\times 1}$. The $3 \times 3$ matrix $Y_F$ is the "regressor matrix," whose exact mathematical expression can be easily obtained using symbolic math packages, and can be constructed from the measurements of $\boldsymbol{\sigma}$ and $\dot{\boldsymbol{\sigma}}$. Similarly, $G^{*\Delta}$ can be written as

$$G^{*\Delta} = Y_G\Theta_G \tag{22}$$

where $\Theta_G$ is a $12N \times 2N$ matrix defined by

$$\Theta_G \triangleq \mathrm{diag}[\Theta_{G1,}\Theta_{G2,}\ldots, \Theta_{G2N}] \in \mathbb{R}^{12N\times 2N} \tag{23}$$

and

$$\Theta_{Gi} \triangleq [\theta_{i,1,}..., \theta_{i,6}]^{\mathrm{T}} \triangleq I_{\mathrm{ws},i}[\mathbf{t}_{i,0}^{\mathrm{T}}, \mathbf{s}_{i,0}^{\mathrm{T}}]^{\mathrm{T}} - I_{\mathrm{ws},i}^{\mathrm{n}}[\mathbf{t}_{i,0}^{\mathrm{nT}}, \mathbf{s}_{i,0}^{\mathrm{nT}}]^{\mathrm{T}}, \quad i = 1,\ldots,N \tag{24a}$$

$$\Theta_{G(i+N)} \triangleq [\theta_{i+N,1,}..., \theta_{i+N,6}]^{\mathrm{T}} \triangleq I_{\mathrm{ws},i}[\mathbf{t}_{i,0}^{\mathrm{T}}, \mathbf{s}_{i,0}^{\mathrm{T}}]^{\mathrm{T}} - I_{\mathrm{ws},i}^{\mathrm{n}}[\mathbf{t}_{i,0}^{\mathrm{nT}}, \mathbf{s}_{i,0}^{\mathrm{nT}}]^{\mathrm{T}}, \quad i = 1,\ldots,N \tag{24b}$$

The vectors $\mathbf{t}_{i,0}$, $\mathbf{t}_{i,0}^{\mathrm{n}}$, $\mathbf{s}_{i,0}$ and $\mathbf{s}_{i,0}^{\mathrm{n}}$ are the $i$th columns of the matrices $A_{\mathrm{t}0}$, $A_{\mathrm{t}0}^{\mathrm{n}}$, $A_{\mathrm{s}0}$ and $A_{\mathrm{s}0}^{\mathrm{n}}$, respectively. Notice that according to the previous definition, $\Theta_{Gi}$ and $\Theta_{G(i+1)}$ have the same physical meaning but they will be estimated separately, since they are related to different control inputs $\dot{\gamma}_i$ and $\dot{\Omega}_i$, respectively. The regression matrix $Y_G$ is a $3 \times 12N$ matrix defined by

$$Y_G \triangleq [Y_{G1}, Y_{G2},\ldots, Y_{G2N}] \in \mathbb{R}^{3\times 12N} \tag{25}$$

where

$$Y_{Gi} \triangleq -H^{*-1}G^{-\mathrm{T}}\Omega_i[I\cos\gamma_{i,} - I\sin\gamma_i] \in \mathbb{R}^{3\times 6}, \quad i = 1,\ldots,N \tag{26a}$$

$$Y_{G(i+N)} \triangleq -H^{*-1}G^{-\mathrm{T}}[I\sin\gamma_{i,} I\cos\gamma_i] \in \mathbb{R}^{3\times 6}, \quad i = 1,\ldots,N \tag{26b}$$

## Adaptive Controller Design

Assume that the attitude to be tracked is given in terms of some known bounded functions $\boldsymbol{\sigma}_d(t)$, $\dot{\boldsymbol{\sigma}}_d(t)$ and $\ddot{\boldsymbol{\sigma}}_d(t)$ for $t \geq 0$. Here $\boldsymbol{\sigma}_d$ is the MRP vector representing the attitude of a desired reference frame ($\mathcal{D}$-frame) with respect to the inertial frame ($\mathcal{I}$-frame). Defining the error

$$\mathbf{e} \triangleq \begin{bmatrix} \boldsymbol{\sigma}_e \\ \dot{\boldsymbol{\sigma}}_e \end{bmatrix} = \begin{bmatrix} \boldsymbol{\sigma} - \boldsymbol{\sigma}_d \\ \dot{\boldsymbol{\sigma}} - \dot{\boldsymbol{\sigma}}_d \end{bmatrix} \tag{27}$$

one obtains the tracking error dynamics from equation (14) as

$$\dot{\mathbf{e}} = A_0\mathbf{e} + B(F^*(\boldsymbol{\sigma}, \dot{\boldsymbol{\sigma}}) + G^*(\boldsymbol{\sigma}, \boldsymbol{\gamma}, \boldsymbol{\Omega})\boldsymbol{u} - \ddot{\boldsymbol{\sigma}}_d) \tag{28}$$

where

$$A_0 \triangleq \begin{bmatrix} 0 & I \\ 0 & 0 \end{bmatrix}, \quad B \triangleq \begin{bmatrix} 0 \\ I \end{bmatrix} \tag{29}$$

It can be easily shown that the pair $(A_0, B)$ is controllable, so one can choose a gain matrix $K$ such that $A \triangleq A_0 - BK$ is Hurwitz, and rewrite (28) as

$$\dot{\mathbf{e}} = A\mathbf{e} + B(K\mathbf{e} + F^*(\boldsymbol{\sigma}, \dot{\boldsymbol{\sigma}}) + G^*(\boldsymbol{\sigma}, \boldsymbol{\gamma}, \boldsymbol{\Omega})\boldsymbol{u} - \ddot{\boldsymbol{\sigma}}_d) \tag{30}$$

Now let $P = P^{\mathrm{T}} > 0$ be a solution to the Lyapunov equation

$$A^{\mathrm{T}}P + PA + R = 0, \quad R = R^{\mathrm{T}} > 0 \tag{31}$$

and choose a Lyapunov function candidate as

$$V(\mathbf{e}, \tilde{\Theta}_F, \tilde{\Theta}_G) \triangleq \frac{1}{2}\mathbf{e}^{\mathrm{T}}P\mathbf{e} + \frac{1}{2\alpha_F}\tilde{\Theta}_F^{\mathrm{T}}\tilde{\Theta}_F + \frac{1}{2\alpha_G}\mathrm{tr}(\tilde{\Theta}_G^{\mathrm{T}}\tilde{\Theta}_G), \quad \alpha_F, \alpha_G > 0 \tag{32}$$

where $\tilde{\Theta}_* \triangleq \hat{\Theta}_* - \Theta_*$, and $\hat{\Theta}_*$ is an estimate of $\Theta_*$ to be determined by the parameter adaptation law.

Since the dynamics $\dot{\mathbf{e}} = A\mathbf{e}$ is asymptotically stable, if the matrices $F^*(\boldsymbol{\sigma}, \dot{\boldsymbol{\sigma}})$ and $G^*(\boldsymbol{\sigma}, \boldsymbol{\gamma}, \boldsymbol{\Omega})$ were completely known, one could choose $\boldsymbol{u}$ to cancel the extra terms in (30), that is

$$G^*(\boldsymbol{\sigma}, \boldsymbol{\gamma}, \boldsymbol{\Omega})\boldsymbol{u} = -K\mathbf{e} - F^*(\boldsymbol{\sigma}, \dot{\boldsymbol{\sigma}}) + \ddot{\boldsymbol{\sigma}}_d \tag{33}$$

to obtain the asymptotically stable error system $\dot{\mathbf{e}} = A\mathbf{e}$. However, since $F^*(\boldsymbol{\sigma}, \dot{\boldsymbol{\sigma}})$ and $G^*(\boldsymbol{\sigma}, \boldsymbol{\gamma}, \boldsymbol{\Omega})$ are not known, we will use (18) and replace (33) with its best estimate, that is

$$(G^{*\mathrm{n}} + Y_G\hat{\Theta}_G)\boldsymbol{u} = -K\mathbf{e} - (F^{*\mathrm{n}} + Y_F\hat{\Theta}_F) + \ddot{\boldsymbol{\sigma}}_d \tag{34}$$

If we have at least two wheels ($N \geq 2$), the solution to (34) exists as long as the $3 \times 2N$ matrix $(G^{*\mathrm{n}} + Y_G\hat{\Theta}_G)$ has full row rank. In this case, the (weighted) minimum norm solution is given by

$$\boldsymbol{u} = (G^{*\mathrm{n}} + Y_G\hat{\Theta}_G)^+(-K\mathbf{e} - F^{*\mathrm{n}} - Y_F\hat{\Theta}_F + \ddot{\boldsymbol{\sigma}}_d) \tag{35}$$

where $(\bullet)^+$ denotes the (weighted) pseudo-inverse[5] of a matrix [8]. Using (18), along with (21) and (22), the tracking error dynamics in (28) can be written as

$$\begin{aligned} \dot{\mathbf{e}} &= A\mathbf{e} + B(K\mathbf{e} + F^{*\mathrm{n}} + F^{*\Delta} + (G^{*\mathrm{n}} + G^{*\Delta})\boldsymbol{u} - \ddot{\boldsymbol{\sigma}}_d) \\ &= A\mathbf{e} + B(K\mathbf{e} + F^{*\mathrm{n}} + Y_F\Theta_F + (G^{*\mathrm{n}} + Y_G\Theta_G)\boldsymbol{u} - \ddot{\boldsymbol{\sigma}}_d) \\ &= A\mathbf{e} + B(K\mathbf{e} + F^{*\mathrm{n}} + Y_F(\hat{\Theta}_F - \tilde{\Theta}_F) + (G^{*\mathrm{n}} + Y_G\hat{\Theta}_G)\boldsymbol{u} - Y_G\tilde{\Theta}_G\boldsymbol{u} - \ddot{\boldsymbol{\sigma}}_d) \end{aligned} \tag{36}$$

[5]The weighted pseudo-inverse of a matrix $Q$ is given by $W^{\frac{1}{2}}(QW^{\frac{1}{2}})^+$, where $(\bullet)^+$ denotes the Moore-Penrose inverse. The use of the weight matrix $W$ is included to smoothly switch between CMG and reaction-wheel modes; see reference [8].

Using (34), the previous equation yields

$$\dot{\mathbf{e}} = A\mathbf{e} - BY_F\tilde{\Theta}_F - BY_G\tilde{\Theta}_G\boldsymbol{u} \tag{37}$$

The time derivative of $V$ then becomes

$$\begin{aligned}\dot{V} &= \frac{1}{2}\mathbf{e}^{\mathrm{T}}(A^{\mathrm{T}}P + PA)\mathbf{e} - \mathbf{e}^{\mathrm{T}}PBY_F\tilde{\Theta}_F - \mathbf{e}^{\mathrm{T}}PBY_G\tilde{\Theta}_G\boldsymbol{u} + \frac{1}{\alpha_F}\dot{\hat{\Theta}}_F\tilde{\Theta}_F + \frac{1}{\alpha_G}\mathrm{tr}(\dot{\hat{\Theta}}_G\tilde{\Theta}_G) \\ &= -\frac{1}{2}\mathbf{e}^{\mathrm{T}}R\mathrm{e} + \frac{1}{\alpha_F}\tilde{\Theta}_F^{\mathrm{T}}(\dot{\hat{\Theta}}_F - \alpha_F Y_F^{\mathrm{T}}B^{\mathrm{T}}P\mathbf{e}) + \frac{1}{\alpha_G}\mathrm{tr}[\tilde{\Theta}_G^{\mathrm{T}}(\dot{\hat{\Theta}}_G - \alpha_G Y_G^{\mathrm{T}}B^{\mathrm{T}}P\mathbf{e}\boldsymbol{u}^{\mathrm{T}})] \qquad (38) \\ &= -\frac{1}{2}\mathbf{e}^{\mathrm{T}}R\mathrm{e} + \frac{1}{\alpha_F}\tilde{\Theta}_F^{\mathrm{T}}(\dot{\hat{\Theta}}_F - \alpha_F Y_F^{\mathrm{T}}B^{\mathrm{T}}P\mathbf{e}) + \frac{1}{\alpha_G}\sum_{i=1}^{2N}\tilde{\Theta}_{Gi}^{\mathrm{T}}(\dot{\hat{\Theta}}_{Gi} - \alpha_G Y_{Gi}^{\mathrm{T}}B^{\mathrm{T}}P\mathbf{e}u_i)\end{aligned}$$

Choosing the parameter adaptation law

$$\dot{\hat{\Theta}}_F = \alpha_F Y_F^{\mathrm{T}}B^{\mathrm{T}}P\mathbf{e} \tag{39}$$

$$\dot{\hat{\Theta}}_{Gi} = \alpha_G Y_{Gi}^{\mathrm{T}}B^{\mathrm{T}}P\mathbf{e}u_i, \quad i = 1, \ldots, 2N \tag{40}$$

results in $\dot{V}(\mathbf{e}, \tilde{\Theta}_F, \tilde{\Theta}_G) = -\frac{1}{2}\mathbf{e}^{\mathrm{T}}R\mathbf{e} \leq 0$. This inequality implies that the tracking error $\mathbf{e}$ and the estimate errors $\tilde{\Theta}_F$ and $\tilde{\Theta}_G$ are bounded. Assuming that all the wheel speeds $\Omega_i$ remain bounded,[6] it can be shown that $\dot{V} \to 0$, and thus $\mathbf{e} \to 0$ as $t \to \infty$ by using Barbalat's lemma and standard arguments [26, 27] (see the Appendix for the details of the proof). We have therefore shown the following proposition.

**Proposition 1.** *Assuming that the matrix* $(G^{*\mathrm{n}} + Y_G\hat{\Theta}_G)$ *has full row rank and that the wheel speeds* $\Omega_i$, $i = 1, \ldots, N$ *remain bounded, the steering law (35), along with the parameter adaptation law (39)–(40) ensures that the error (27) tends to zero as* $t \to \infty$.

*Smooth Parameter Projection*

A drawback of the previous adaptation law (40) is that a drift of the estimate of the parameter $\hat{\Theta}_G$ by (40) can result in the matrix $(G^{*\mathrm{n}} + Y_G\hat{\Theta}_G)$ losing rank. We will refer to this situation as a "singular case" of the steering law due to the adaptation.[7]

If we use more than two VSCMGs with their nominal gimbal axes not parallel to each other, the nominal matrix $G^{*\mathrm{n}}$ has full row rank [12]. Therefore, if the true value of the parameter uncertainty $\Theta_G$ is bounded by a sufficiently small number, and we can also keep its estimated value $\hat{\Theta}_G$ small, then the matrix $(G^{*\mathrm{n}} + Y_G\hat{\Theta}_G)$ will also have full row rank. To this end, we define the two convex sets

$$\Omega_{\Theta_{Gi}} \triangleq \{\Theta_{Gi} \in \mathbb{R}^6 \,|\, \|\Theta_{Gi}\|^2 < \beta_{Gi}\}$$
$$\hat{\Omega}_{\Theta_{Gi}} \triangleq \{\hat{\Theta}_{Gi} \in \mathbb{R}^6 \,|\, \|\hat{\Theta}_{Gi}\|^2 < \beta_{Gi} + \delta_{Gi}\}$$

[6]Boundedness of the wheel speeds can be easily imposed by applying a suitable torque in the null space of the matrix $(G^{*\mathrm{n}} + Y_G\hat{\Theta}_G)$, similarly to the technique used in reference [8]. Such a torque has no effect on attitude tracking performance.

[7]This singularity must be distinguished from the geometric singularity of CMGs in which all of the transverse axes lie on a two-dimensional plane.

where $\beta_{Gi} > 0$ and $\delta_{Gi} > 0$ are known constants. Notice that $\Omega_{\Theta_{Gi}} \subset \hat{\Omega}_{\Theta_{Gi}}$. We make the two assumptions:

- **Assumption 1.** The actual value $\Theta_{Gi}$ belongs to the set $\Omega_{\Theta_{Gi}}$.
- **Assumption 2.** If $\hat{\Theta}_{Gi} \in \hat{\Omega}_{\Theta_{Gi}}$ for all $i = 1, \ldots, 2N$, then $(G^{*\mathrm{n}} + Y_G \hat{\Theta}_G)$ is nonsingular.

The previous assumptions allow us to modify the adaptation law (40) by using the "smooth projection algorithm"[8] as [15–17, 19]

$$\dot{\hat{\Theta}}_{Gi} = \mathrm{Proj}(\hat{\Theta}_{Gi}, \Phi_{Gi}) \quad i = 1, \ldots, 2N \tag{41}$$

where

$$\Phi_{Gi} \triangleq Y_{Gi}^{\mathrm{T}} B^{\mathrm{T}} P \mathbf{e} u_i \tag{42}$$

and

$$\mathrm{Proj}(\hat{\Theta}_{Gi}, \Phi_{Gi}) \triangleq$$

$$\begin{cases} \alpha_G \Phi_{Gi}, & \text{if (i) } \|\hat{\Theta}_{Gi}\|^2 < \beta_{Gi}, \text{ or} \\ & \quad \text{(ii) } \|\hat{\Theta}_{Gi}\|^2 \geq \beta_{Gi} \text{ and } \Phi_{Gi}^{\mathrm{T}} \hat{\Theta}_{Gi} \leq 0 \\ \alpha_G \left( \Phi_{Gi} - \dfrac{(\|\hat{\Theta}_{Gi}\|^2 - \beta_{Gi}) \Phi_{Gi}^{\mathrm{T}} \hat{\Theta}_{Gi}}{\delta_{Gi} \|\hat{\Theta}_{Gi}\|^2} \hat{\Theta}_{Gi} \right) & \\ & \text{if (iii) } \|\hat{\Theta}_{Gi}\|^2 \geq \beta_{Gi} \text{ and } \Phi_{Gi}^{\mathrm{T}} \hat{\Theta}_{Gi} > 0 \end{cases} \tag{43}$$

This adaptation law is identical to (40) in Cases (i) and (ii), and switches smoothly to a new expression in Case (iii). The projection operator $\mathrm{Proj}(\hat{\Theta}_{Gi}, \Phi_{Gi})$ is locally Lipschitz in $(\hat{\Theta}_{Gi}, \Phi_{Gi})$, thus the system has a unique solution defined for some time interval $[0, T)$, $T > 0$.

**Proposition 2.** *Under Assumptions 1 and 2, and assuming that the wheel speeds $\Omega_i$, $i = 1, \ldots, N$ remain bounded, the steering law equation (35) along with the adaptation laws equations (39) and (41) yields*

$$\dot{V}(\mathbf{e}, \tilde{\Theta}_F, \tilde{\Theta}_G) \leq -\frac{1}{2} \mathbf{e}^{\mathrm{T}} R \mathbf{e} \tag{44}$$

*and*

$$\hat{\Theta}_{Gi}(t = 0) \in \boldsymbol{\Omega}_{\Theta_{Gi}} \Rightarrow \hat{\Theta}_{Gi}(t) \in \hat{\boldsymbol{\Omega}}_{\Theta_{Gi}}, \quad \forall t \geq 0 \tag{45}$$

*Proof.* First, it must be verified that the adaptation rule (41) satisfies

$$\tilde{\Theta}_{Gi}^{\mathrm{T}} (\dot{\hat{\Theta}}_{Gi} - \alpha_G \Phi_{Gi}) \leq 0 \tag{46}$$

which yields (44). In Cases (i) and (ii) the equality in equation (46) trivially holds. In Case (iii), the left hand side of (46) becomes

[8]The adaptation law is, in fact, only Lipschitz continuous, not continuously differentiable. The use of the term "smooth" is a slight misnomer in this context, but we use it here in accordance to prior usage in the literature. It should be noted that a new parameter projection operator which is $C^n$ has been recently introduced in reference [28].

$$\tilde{\Theta}_{Gi}^{\mathrm{T}}(\dot{\hat{\Theta}}_{Gi} - \alpha_G \Phi_{Gi}) = -\alpha_G \frac{(\|\hat{\Theta}_{Gi}\|^2 - \beta_{Gi})\Phi_{Gi}^{\mathrm{T}}\hat{\Theta}_{Gi}}{\delta_{Gi}\|\hat{\Theta}_{Gi}\|^2}\,\tilde{\Theta}_{Gi}^{\mathrm{T}}\hat{\Theta}_{Gi} \le 0 \tag{47}$$

because $\tilde{\Theta}_{Gi}^{\mathrm{T}}\hat{\Theta}_{Gi} \ge 0$ when $\|\hat{\Theta}_{Gi}\|^2 \ge \beta_{Gi}$ as shown in Fig. 2. Thus, it is shown that equation (44) holds.

Now, let us show that the condition (45) holds. In Case (i) it trivially holds because $\hat{\Theta}_{Gi} \in \Omega_{\Theta_{Gi}} \subset \hat{\Omega}_{\Theta_{Gi}}$. In Case (ii), $\dot{\hat{\Theta}}_{Gi}^{\mathrm{T}}\hat{\Theta}_{Gi} = \alpha_G \Phi_{Gi}^{\mathrm{T}}\hat{\Theta}_{Gi} \le 0$, thus the estimate $\hat{\Theta}_{Gi}$ moves closer to zero. In Case (iii)

$$\dot{\hat{\Theta}}_{Gi}^{\mathrm{T}}\hat{\Theta}_{Gi} = \alpha_G \Phi_{Gi}^{\mathrm{T}}\hat{\Theta}_{Gi}\left(1 - \frac{(\|\hat{\Theta}_{Gi}\|^2 - \beta_{Gi})}{\delta_{Gi}}\right)\begin{cases} < 0 \text{ if } \|\hat{\Theta}_{Gi}\|^2 > \beta_{Gi} + \delta_{Gi} \\ = 0 \text{ if } \|\hat{\Theta}_{Gi}\|^2 = \beta_{Gi} + \delta_{Gi} \\ > 0 \text{ if } \|\hat{\Theta}_{Gi}\|^2 < \beta_{Gi} + \delta_{Gi} \end{cases} \tag{48}$$

thus $\hat{\Theta}_{Gi}$ does not drift outside the set $\hat{\Omega}_{\Theta_{Gi}}$. □

Equation (44) can be written as $\dot{V} = -\frac{1}{2}\mathbf{e}^{\mathrm{T}}R\mathbf{e} + \zeta(\mathbf{e}, \tilde{\Theta}_G, \Phi_G) \le -\frac{1}{2}\mathbf{e}^{\mathrm{T}}R\mathbf{e}$, where $\zeta(\mathbf{e}, \tilde{\Theta}_G, \Phi_G) \le 0$. Using a similar argument as in the proof of Proposition 1, it can be shown that $\dot{V} = -\frac{1}{2}\mathbf{e}^{\mathrm{T}}R\mathbf{e} + \zeta(\mathbf{e}, \tilde{\Theta}_G, \Phi_G) \to 0$ as $t \to \infty$ and thus $\mathbf{e} \to 0$ because $\zeta(\mathbf{e}, \tilde{\Theta}_G, \Phi_G) \le 0$ (see the Appendix for a detailed proof). Hence, from Proposition 2, one concludes that using the control law (35) and the adaptation laws (39) and (41), one obtains that $\mathbf{e} \to 0$ as $t \to \infty$ and $(G^{*\mathrm{n}} + Y_G\hat{\Theta}_G)$ will not lose rank, if we choose the initial parameter guess $\hat{\Theta}_{Gi}(0)$ inside the set $\Omega_{\Theta_{Gi}}$. For instance, we may take $\hat{\Theta}_{Gi}(0) = 0$.

It is worth mentioning that the adaptation law (41) has the additional benefit of keeping the parameter estimates from bursting. It is well known that parameter estimates do not necessarily converge to their actual values unless persistency of excitation holds. In fact, the estimates can momentarily take very large values ("burst") [30, 31]. Thanks to the smooth projection algorithm, however, the parameter estimates under the proposed adaptation laws will be confined in a convex set even when persistency of excitation does not hold.

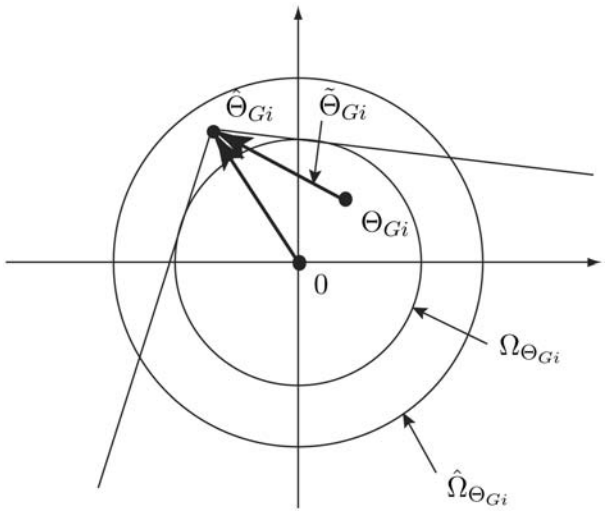


**FIG. 2.** $\tilde{\Theta}_{Gi}^{\mathrm{T}}\hat{\Theta}_{Gi} \ge 0$ in Case (iii).

## Numerical Example

Numerical examples for a satellite with a VSCMG cluster are provided in this section to test the proposed adaptive control algorithm. In this section the complete nonlinear equations of motion, given in equation (1), along with the acceleration steering law derived in reference [8], are used to predict and validate the performance of the proposed controllers under realistic conditions. In addition, the null motion technique presented in reference [11] is also applied, along with the proposed control law, in order to avoid the geometric singularity of VSCMGs. The wheel speeds are bounded using a null torque, as discussed in footnote 6. This torque, being in the null space of the matrix $(G^{*\mathrm{n}} + Y_G\hat{\Theta}_G)$, has no effect on the output torque and hence the stability analysis of the adaptive control laws developed earlier still holds.

The parameters used for the simulations are shown in Table 1. Notice that the initial wheel speeds of the VSCMGs are set to 30,000 RPM, a value that is an order of magnitude larger than the speed of conventional CMGs, since the flywheels of VSCMGs used for IPACS in general need to spin very fast so that they are competitive against traditional chemical batteries. We assume a standard four-VSCMG pyramid configuration, as shown in Fig. 3.

The nominal values of the axis directions at $\boldsymbol{\gamma} = [0, 0, 0, 0]^{\mathrm{T}}$ are

$$A^{\mathrm{n}}_{\mathrm{s}0} = \left[\mathbf{s}^{\mathrm{n}}_{1,0}, \mathbf{s}^{\mathrm{n}}_{2,0}, \mathbf{s}^{\mathrm{n}}_{3,0}, \mathbf{s}^{\mathrm{n}}_{4,0}\right] = \begin{bmatrix} 0 & -1 & 0 & 1 \\ 1 & 0 & -1 & 0 \\ 0 & 0 & 0 & 0 \end{bmatrix} \tag{49}$$

$$A^{\mathrm{n}}_{\mathrm{t}0} = \left[\mathbf{t}^{\mathrm{n}}_{1,0}, \mathbf{t}^{\mathrm{n}}_{2,0}, \mathbf{t}^{\mathrm{n}}_{3,0}, \mathbf{t}^{\mathrm{n}}_{4,0}\right] = \begin{bmatrix} -0.5774 & 0 & 0.5774 & 0 \\ 0 & -0.5774 & 0 & 0.5774 \\ 0.8165 & 0.8165 & 0.8165 & 0.8165 \end{bmatrix} \tag{50}$$

The (unknown) actual axis directions at $\boldsymbol{\gamma} = 0$ used in the present example are assumed as

**TABLE 1. Simulation Parameters**

| Symbol | Value | Units |
|---|---|---|
| $N$ | 4 | – |
| $\theta$ | 54.75 | deg |
| $\boldsymbol{\omega}(0)$ | $[0, 0, 0]^{\mathrm{T}}$ | rad/sec |
| $\dot{\boldsymbol{\omega}}(0)$ | $[0, 0, 0]^{\mathrm{T}}$ | rad/sec$^2$ |
| $\boldsymbol{\sigma}(0)$ | $[0.2153, 0.2153, 0.2153]^{\mathrm{T}}$ | – |
| $\boldsymbol{\gamma}(0)$ | $[0, 0, 0, 0]^{\mathrm{T}}$ | rad |
| $\dot{\boldsymbol{\gamma}}(0)$ | $[0, 0, 0, 0]^{\mathrm{T}}$ | rad/sec |
| $\boldsymbol{\Omega}(0)$ | $3.0 \times 10^4\,[1, 1, 1, 1]^{\mathrm{T}}$ | rpm |
| $B_I$ | $\begin{bmatrix} 15000 & 3000 & -1000 \\ 3000 & 6500 & 2000 \\ -1000 & 2000 & 12000 \end{bmatrix}$ | kg m$^2$ |
| $I_{\mathrm{wt}}, I_{\mathrm{wg}}$ | diag$\{0.4, 0.4, 0.4, 0.4\}$ | kg m$^2$ |
| $I_{\mathrm{gs}}, I_{\mathrm{wg}}, I_{gg}$ | diag$\{0.1, 0.1, 0.1, 0.1\}$ | kg m$^2$ |

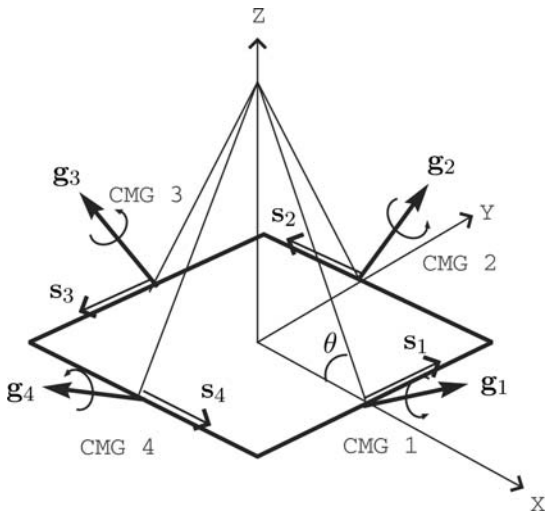


**FIG. 3.** A VSCMG System with Pyramid Configuration at $\boldsymbol{\gamma} = [0, 0, 0, 0]^{\mathrm{T}}$.

$$A_{s0} = [\mathbf{s}_{1,0}, \mathbf{s}_{2,0}, \mathbf{s}_{3,0}, \mathbf{s}_{4,0}] = \begin{bmatrix} 0.0192 & -0.9984 & -0.0396 & 0.9984 \\ 0.9990 & -0.0404 & -0.9990 & -0.0396 \\ -0.0404 & -0.0396 & -0.0208 & -0.0404 \end{bmatrix} \quad (51)$$

$$A_{t0} = [\mathbf{t}_{1,0}, \mathbf{t}_{2,0}, \mathbf{t}_{3,0}, \mathbf{t}_{4,0}] = \begin{bmatrix} -0.5438 & -0.0101 & 0.5435 & 0.0556 \\ 0.0443 & -0.5611 & -0.0390 & 0.5598 \\ 0.8380 & 0.8277 & 0.8385 & 0.8268 \end{bmatrix} \quad (52)$$

which are obtained by slightly perturbing the nominal axis directions. This choice of perturbation leads to orthogonality of the axes for the uncertain matrices as well. In contrast, arbitrary perturbations of the elements of the nominal matrices $A_{s0}^{n}$ and $A_{t0}^{n}$ are not physically meaningful since they may not preserve the orthogonality of the gimbal axes system.

The nominal and the (unknown) actual values of the moments of inertia of the flywheels along their spin axes are

$$I_{ws}^{n} = \mathrm{diag}\{2.0, 2.0, 2.0, 2.0\} \text{ kg m}^2 \quad (53)$$

$$I_{ws} = \mathrm{diag}\{1.98, 2.01, 2.02, 1.99\} \text{ kg m}^2 \quad (54)$$

respectively. The feedback gain $K$ in (30) is chosen so that the eigenvalues of the matrix $A = A_0 - BK$ are given by

$$\mathrm{eig}(A) = \left\{-0.2 \pm 0.2i, -0.2\sqrt{2}, -0.3 \pm 0.3i, -0.3\sqrt{2}\right\}$$

The remaining design parameters for the adaptive control law are chosen as

$$R = 1.0 \times 10^3 I, \quad \beta_F = 1.5 \times 10^6, \quad \delta_F = 1.0 \times 10^5, \quad \beta_{Gi} = 0.1, \quad \delta_{Gi} = 0.05$$
$$\alpha_F = 1.0 \times 10^6, \quad \alpha_G = 5.0 \times 10^1$$

The reference trajectory is chosen so that the initial reference attitude is aligned with the inertial frame, that is $\boldsymbol{\sigma}_d(0) = [0, 0, 0]^{\mathrm{T}}$, and the angular velocity of the reference attitude is chosen as

$$\omega_d(t) = (0.04\sin(2\pi t/400),\ 0.04\sin(2\pi t/300),\ 0.04\sin(2\pi t/200))^{\mathrm{T}}\ \mathrm{rad/sec} \quad (55)$$

The initial attitude, angular rate, and angular acceleration of the spacecraft are given in Table 1.

First, and in order to justify the use of the simplified equations of motion during the controller design step, we ran a simulation with the full dynamic equations with no uncertainty. That is, we assumed that $A_{s0} = A^{n}_{s0}$ and $A_{t0} = A^{n}_{t0}$. Recall that the controller was designed based on the simplified set of the equations of motion (5)–(7). Figure 4(a) shows the steady-state attitude error expressed with 3-2-1 Euler angles.[9] This error reflects the effect of the neglected dynamics with the aforementioned assumptions of $\dot{J} = 0$, $A_s I_{cg}\dot{\boldsymbol{\gamma}} = 0$, and $A_s I_{cg}\ddot{\boldsymbol{\gamma}} = 0$. The level of the attitude error is shown to be less than 0.002 deg, which is practically negligible. From this observation, we are assured that the neglected dynamics do not have a major impact on the attitude behavior of the spacecraft.

Next, in order to show the effect of the misalignment of the axes of the VSCMG cluster and the uncertainty in the flywheel inertias, we performed a simulation using the full dynamic equations, with uncertainties but without adaptation. Figure 4(b) shows the attitude error under the control law with the adaptation gains $\alpha_F$ and $\alpha_G$ set to zero. Comparing Figs. 4(a) and 4(b), one confirms that the effect of the uncertainties is three orders of magnitude larger than that of the neglected dynamics, and thus this is the dominant cause of the tracking error. We can therefore justify the use of the simplified equations in the control algorithm design stage.

Figure 5 shows the simulation results using the designed adaptive control law. As shown in Figure 5(a), a residual persistent error is observed because the controller is designed based on the simplified equations of motion, which have neglected several (secondary) effects, while the full equations of motion are used for the numerical simulations. Nonetheless, the attitude error is significantly attenuated using the adaptive controller (compare with Fig. 4(b)). When the algorithm is applied to the simplified equations, the error indeed tends to zero as predicted by the theory (see Fig. 5(b)).

Figure 6 shows the time history of the parameter estimate $\hat{\Theta}_F$. The bold horizontal dotted lines denote the actual values of the components of $\Theta_F$. The estimates

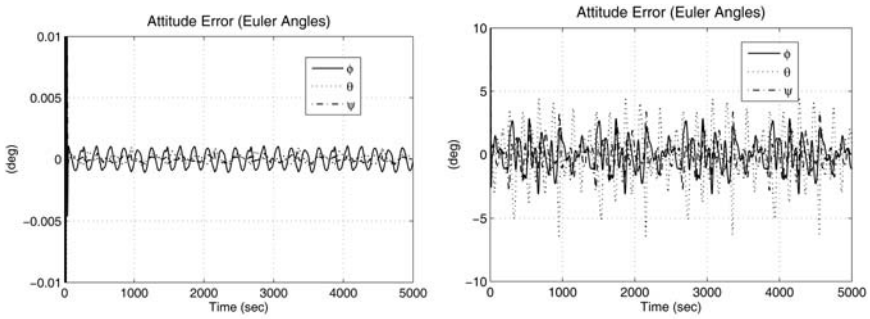


(a) Without Uncertainties (b) With Uncertainties but Without Adaptation

**FIG. 4.** The Steady-State Attitude Errors.

[9]The use of Euler angles in the figures is done solely for the convenience of the reader who may not be familiar with the MRPs.

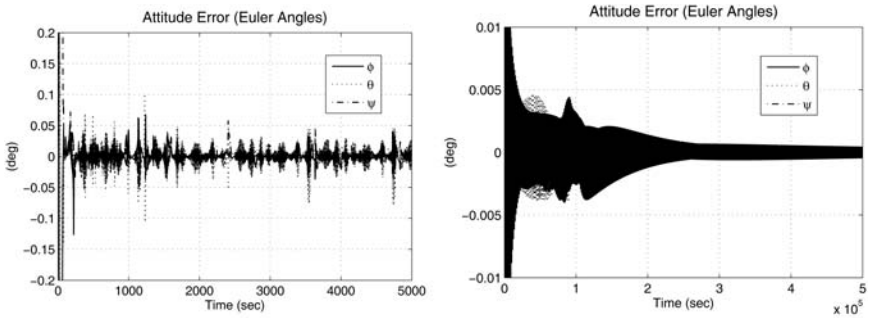


(a) Using Exact Equations (b) Using Simplified Equations

**FIG. 5.** The Attitude Error with Adaptation.

approach the actual values, but they do not exactly converge to these values due to the lack of persistency of excitation. Note that, in general—and for a linear system—convergent estimation of $m$ parameters requires at least $m/2$ sinusoids in the reference signal. For the nonlinear case such a simple relation may not be valid [27]. In this example, the number of the parameters to be estimated is $12N + 3$, while the reference signal has only three sinusoids, thus the persistency condition is not satisfied. Figure 7 shows the time history of $\|\hat{\Theta}_{Gi}\|^2$. Similarly to $\hat{\Theta}_F$, the estimates of $\hat{\Theta}_{Gi}$ do not converge to the actual values due to the lack of persistency of excitation. However, it is confirmed that the $\|\hat{\Theta}_{Gi}\|^2$ do not drift more than $\beta_{Gi} + \delta_{Gi} = 0.15$ owing to the smooth projection algorithm in (43). As a result, the steering law (35) remains well-defined. Finally, the states of the VSCMG cluster are shown in Fig. 8.

## Conclusions

In this paper, we propose an adaptive tracking control law for the attitude of a rigid spacecraft when the exact directions of the torque-generating axes and the moment of inertia of a Variable Speed Control Moment Gyro (VSCMG) cluster are unknown or uncertain. Although the control law is designed using a simplified set

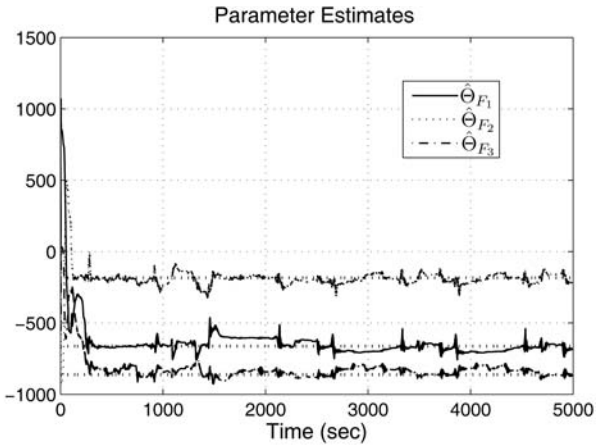


**FIG. 6.** Parameter Estimate $\hat{\Theta}_F$.

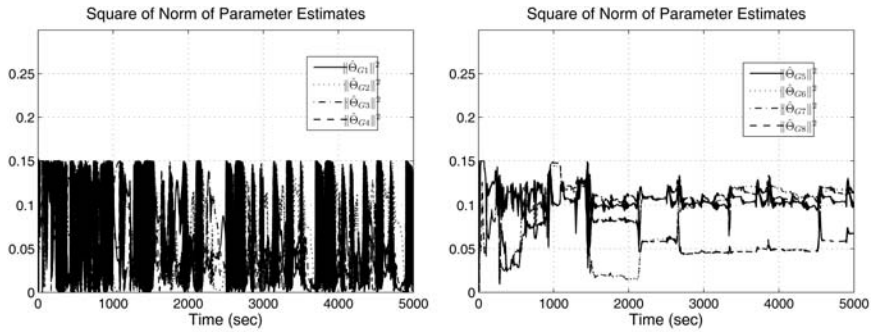


(a) $i = 1, 2, 3, 4$ (b) $i = 5, 6, 7, 8$

**FIG. 7.** Square of Norms of Parameter Estimate $\|\hat{\Theta}_{Gi}\|^2$.

of equations of motion, the numerical examples indicate that the control law works exceedingly well when applied to the complete set of equations. Furthermore, the adaptive law confines the parameter estimates inside a user-defined convex set, which is assumed to contain the unknown actual values. This prevents parameter "bursting," a well-known behavior of general adaptive control laws when persistency of excitation does not hold. Since the present article provides a first step towards the general solution of spacecraft control with actuator misalignment/uncertainties, several extensions and improvements are possible over the baseline control logic proposed in this paper. For instance, one can include the effect of the (unknown) inertia matrix. This problem can be dealt with easily (but conservatively) using an over-parameterization. Depending on the number of uncertainties present in the problem (actuator axes and/or moment of inertia entries, etc) the number of parameters to be adapted may increase significantly. In that sense, methods for reducing the overall number of estimated parameters would be extremely beneficial.

**Acknowledgment**

Support for this work was provided from AFOSR award F49620-001-0374.

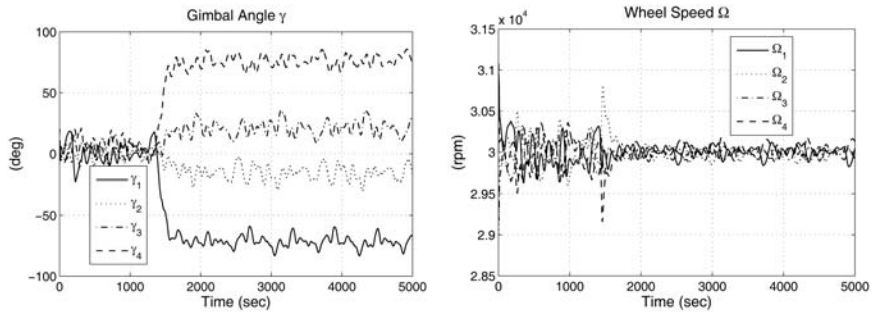


(a) Gimbal angle $\boldsymbol{\gamma}$ (b) Wheel Speed $\boldsymbol{\Omega}$

**FIG. 8.** Gimbal Angle $\boldsymbol{\gamma}$ and Wheel Speed $\boldsymbol{\Omega}$.

## References


[1] SLOTINE, J. J. E. and BENEDETTO, M. D. D. "Hamiltonian Adaptive Control of Spacecraft," *IEEE Transactions on Automatic Control*, Vol. 35, July 1990, pp. 848–852.

[2] BISHOP, R., PAYNTER, S., and SUNKEL, J. "Adaptive Control of Space Station with Control Moment Gyros," *IEEE Control Systems Magazine*, Vol. 12, October 1992, pp. 23–28.

[3] SHEEN, J. and BISHOP, R. "Adaptive Nonlinear Control of Spacecraft," *Proceedings of the American Control Conference*, Baltimore, Maryland, 1994, pp. 2867–2871.

[4] ZAREMBA, A. "An Adaptive Scheme with Parameter Identification for Spacecraft Attitude Control," *Proceedings of the American Control Conference*, 1997, pp. 552–556.

[5] AHMED, J. and BERNSTEIN, D. "Adaptive Control of a Dual-Axis CMG with an Unbalanced Rotor," *Proceedings of the 37th IEEE Conference on Decision and Control*, Tampa, FL, December 1992, pp. 4531–4536.

[6] AHMED, J., COPPOLA, V., and BERNSTEIN, D. "Adaptive Asymptotic Tracking of Spacecraft Attitude Motion with Inertia Matrix Identification," *Journal of Guidance, Control, and Dynamics*, Vol. 21, No. 5, 1998, pp. 684–691.

[7] SCHAUB, H., AKELLA, M. R., and JUNKINS, J. L. "Adaptive Realization of Linear Closed-Loop Tracking Dynamics in the Presence of Large System Model Errors," *The Journal of the Astronautical Sciences*, Vol. 48, October–December 2000, pp. 537–551.

[8] YOON, H. and TSIOTRAS, P. "Spacecraft Adaptive Attitude and Power Tracking with Variable Speed Control Moment Gyroscopes," *Journal of Guidance, Control, and Dynamics*, Vol. 25, November–December 2002, pp. 1081–1090.

[9] LEVEDEV, D. V. and TKACHENKO, A. I. "High-Accurate Stabilization of a Spacecraft with Incomplete Actuators," *Journal of Automation and Information Sciences*, Vol. 31, No. 4, 1999, pp. 75–84.

[10] TSIOTRAS, P., SHEN, H., and HALL, C. "Satellite Attitude Control and Power Tracking with Energy/Momentum Wheels," *Journal of Guidance, Control, and Dynamics*, Vol. 24, No. 1, 2001, pp. 23–34.

[11] YOON, H. and TSIOTRAS, P. "Singularity Analysis of Variable-Speed Control Moment Gyros," *Journal of Guidance, Control, and Dynamics*, Vol. 27, No. 3, 2004, pp. 374–386.

[12] SCHAUB, H., VADALI, S. R., and JUNKINS, J. L. "Feedback Control Law for Variable Speed Control Moment Gyroscopes," *The Journal of the Astronautical Sciences*, Vol. 46, No. 3, 1998, pp. 307–328.

[13] SLOTINE, J.-J. E. and LI, W. "Adaptive Manipulator Control: A Case Study," *IEEE Transactions on Automatic Control*, Vol. 33, November 1988, pp. 995–1003.

[14] GE, S. S. "Adaptive Control of Robots Having both Dynamical Parameter Uncertainties and Unknown Input Scalings," *Mechatronics*, Vol. 6, No. 5, 1996, pp. 557–569.

[15] CHANG, Y.-C. "An Adaptive $\mathcal{H}_\infty$ Tracking Control for a Class of Nonlinear Multiple-Input-Multiple-Output (MIMO) Systems," *IEEE Transactions on Automatic Control*, Vol. 46, September 2001, pp. 1432–1437.

[16] POMET J.-B. and PRALY, L. "Adaptive Nonlinear Regulation : Estimation from the Lyapunov Equation," *IEEE Transactions on Automatic Control*, Vol. 37, June 1992, pp. 729–740.

[17] KHALIL, H. K. "Adaptive Output Feedback Control of Nonlinear Systems Represented by Input-Output Models," *IEEE Transactions on Automatic Control*, Vol. 41, February 1996, pp. 177–188.

[18] RICHIE, D., TSIOTRAS, P., and FAUSZ, J. "Simultaneous Attitude Control and Energy Storage Using VSCMGs: Theory and Simulation," in *Proceedings of the American Control Conference*, Arlington, VA, June 25–27, 2001, pp. 3973–3979.

[19] YOON, H. *Spacecraft Attitude and Power Control Using Variable Speed Control Moment Gyros*, Ph.D. Dissertation, Georgia Institute of Technology, Atlanta, GA, December 2004. (URL:http://hdl.handle.net/1853/4850).

[20] FORD, K. A. and HALL, C. D. "Flexible Spacecraft Reorientations Using Gimbaled Momentum Wheels," in *Advances in the Astronautical Sciences, Astrodynamics* (F. Hoots, B. Kaufman, P. J. Cefola, and D. B. Spencer, eds.), Vol. 97, 1997, pp. 1895–1914.

[21] RICHIE, D. J., TSIOTRAS, P., and FAUSZ, J. L. "Simultaneous Attitude Control and Energy Storage using VSCMGs: Theory and Simulation," *Proceedings of the American Control Conference*, 2001, pp. 3973–3979.

[22] TSIOTRAS, P. "Stabilization and Optimality Results for the Attitude Control Problem," *Journal of Guidance, Control, and Dynamics*, Vol. 19, No. 4, 1996, pp. 772–779.

[23] SCHAUB, H. and JUNKINS, J. L. "Stereographic Orientation Parameters for Attitude Dynamics: A Generalization of the Rodrigues Parameters," *The Journal of the Astronautical Sciences*, Vol. 44, No. 1, 1996, pp. 1–19.
[24] SHUSTER, M. D. "A Survey of Attitude Representations," *The Journal of the Astronautical Sciences*, Vol. 41, No. 4, 1993, pp. 439–517.
[25] TSIOTRAS, P., JUNKINS, J. L., and SCHAUB, H. "Higher Order Cayley-Transforms with Applications to Attitude Representations," *Journal of Guidance, Control, and Dynamics*, Vol. 20, No. 3, 1997, pp. 528–534.
[26] KHALIL, H. K. *Nonlinear Systems*, New Jersey: Prentice Hall, 2nd ed., 1996.
[27] SLOTINE, J. and LI, W. *Applied Nonlinear Control*, New Jersey: Prentice Hall, 1991.
[28] CAI, Z., QUEIROZ, M. DE, and DAWSON, D. "A Sufficiently Smooth Projection Operator," *IEEE Transactions on Automatic Control*, Vol. 51, January 2006, pp. 135–139.
[29] KRSTIC, M., KANELLAKOPOULOS, I., and KOKOTOVIC, P. *Nonlinear and Adaptive Control Design,* John Wiley & Sons, 1995.
[30] ANDERSON, B. D. O. "Adaptive Systems, Lack of Persistency of Excitation and the Bursting Phenomenon," *Automatica*, Vol. 21, 1985, pp. 247–258.
[31] ANDERSON, B. D. O. "Failures of Adaptive Control Theory and their Resolution," *Communications in Information and Systems*, Vol. 5, No. 1, 2005, pp. 1–20.
[32] BARTLE, R. G. *The Elements of Real Analysis,* New Jersey: John Whiley & Sons, Inc., 2nd ed., 1976.

## Appendix

*Proof of Proposition 1*

First we provide the details of the proof of Proposition 1.

Assuming that the matrix $(G^{*\mathrm{n}} + Y_G\hat{\Theta}_G)$ is full row rank, the steering law equation (35) is well-defined, and the Lyapunov function $V$ is differentiable. Furthermore, since $V$ is lower bounded and $\dot{V} \leq 0$, if follows that $V(t)$ converges to a limit as $t \to \infty$. In order to prove $\dot{V} \to 0$ as $t \to \infty$, we need only to show that $\dot{V}$ is differentiable and that $\ddot{V}$ is bounded. The latter will ensure that $\dot{V}$ is uniformly continuous (see, for instance, [27]).

Assuming that the matrix $(G^{*\mathrm{n}} + Y_G\hat{\Theta}_G)$ is full row rank, equation (35) results in a well-defined control input. It follows that the expression $\dot{V} = -\frac{1}{2}\mathbf{e}^{\mathrm{T}}R\mathbf{e}$ is differentiable, and its derivative $\ddot{V}(t)$ can be calculated as

$$\ddot{V} = -\mathbf{e}^{\mathrm{T}}R\dot{\mathbf{e}} = -\mathbf{e}^{\mathrm{T}}R(A\mathbf{e} - BY_F\tilde{\Theta}_F - BY_G\tilde{\Theta}_G\boldsymbol{u}) \tag{56}$$

Since $V$ is bounded, it follows that $\mathbf{e}$, $\tilde{\Theta}_F$,and $\tilde{\Theta}_G$ are bounded. It suffices to show that $Y_F, Y_G$, and $\boldsymbol{u}$ are bounded as well. First, notice that since $\boldsymbol{\sigma}_d$ and $\dot{\boldsymbol{\sigma}}_d$ are assumed to be bounded, from equation (27) and the boundedness of $\mathbf{e}$, it follows that $\boldsymbol{\sigma}$ and $\dot{\boldsymbol{\sigma}}$ are bounded. Since $Y_F\Theta_F = F^{*\Delta} = -H^{*-1}(G^{-\mathrm{T}}\boldsymbol{\omega}^{\times}(R_I^{\mathcal{B}}(\boldsymbol{\sigma})\mathbf{H}_I^{\Delta}))$ and $\Theta_F = \mathbf{H}_I^{\Delta}$, $Y_F$ is a product of $H^{*-1}(\boldsymbol{\sigma})$, $G^{-\mathrm{T}}(\boldsymbol{\sigma})$, $\boldsymbol{\omega}^{\times}$, and $R_I^{\mathcal{B}}(\boldsymbol{\sigma})$. Since $\boldsymbol{\sigma}$ is bounded, both $G(\sigma)$ and $G^{-1}(\sigma)$ are bounded, and thus $H^{*-1}(\boldsymbol{\sigma})$, and $G^{-\mathrm{T}}(\boldsymbol{\sigma})$ are bounded as well. It is obvious that the rotational matrix $R_I^{\mathcal{B}}(\boldsymbol{\sigma})$ is bounded, and $\boldsymbol{\omega}$ is also bounded because $\dot{\boldsymbol{\sigma}}$ is bounded. Therefore, $Y_F$ is bounded. Similarly, $Y_G$ is the product of $H^{*-1}(\boldsymbol{\sigma})$, $G^{-\mathrm{T}}(\boldsymbol{\sigma})$, $\boldsymbol{\Omega}$, and some sinusoidal functions (which are bounded), so it is also bounded. Finally, the control input $\boldsymbol{u} = (G^{*\mathrm{n}} + Y_G\hat{\Theta}_G)^{+}(-K\mathbf{e} - F^{*\mathrm{n}} - Y_F\hat{\Theta}_F + \ddot{\boldsymbol{\sigma}}_d)$ is bounded because the matrix $(G^{*\mathrm{n}} + Y_G\hat{\Theta}_G)$ is assumed to have full row rank, $F^{*\mathrm{n}}$ is bounded since $\boldsymbol{\sigma}$, $\dot{\boldsymbol{\sigma}}$, $\boldsymbol{\omega}$ are all bounded, $\mathbf{e}$ and $\hat{\Theta}_F$ have been shown to be bounded (the latter since $\hat{\Theta}_F$ is bounded), and $\ddot{\boldsymbol{\sigma}}_d$ is assumed to be bounded. Therefore, using Barbalat's Lemma [26, 27], it follows that $\dot{V} \to 0$ and thus $\mathbf{e} \to 0$ as $t \to \infty$.

*Proof of Proposition 2*

We can repeat similar arguments to complete the details of the proof of Proposition 2. First, notice that the steering law equation (35) along with the adaptation laws equations (39) and (41), yield for the derivative of $V$

$$\dot{V} = -\frac{1}{2}\,\mathbf{e}^{\mathrm{T}} R\mathbf{e} + \zeta(\mathbf{e}, \tilde{\Theta}_G, \Phi_G) = -\frac{1}{2}\,\mathbf{e}^{\mathrm{T}} R\mathbf{e} + \sum_{i=1}^{N} \zeta_i(\mathbf{e}, \tilde{\Theta}_{Gi}, \Phi_{Gi}) \tag{57}$$

where

$$\zeta_i(\mathbf{e}, \tilde{\Theta}_{Gi}, \Phi_{Gi}) = \begin{cases} 0, & \text{in cases of (i) and (ii)} \\ -\dfrac{(\|\hat{\Theta}_{Gi}\|^2 - \beta_{Gi})\Phi_{Gi}^{\mathrm{T}}\hat{\Theta}_{Gi}}{\delta_{Gi}\|\hat{\Theta}_{Gi}\|^2}\,\tilde{\Theta}_{Gi}^{\mathrm{T}}\hat{\Theta}_{Gi} \le 0, & \text{in case of (iii)} \end{cases} \tag{58}$$

It has been shown that the parameter estimates $\hat{\Theta}_{Gi}$ do not drift outside the set $\hat{\Omega}_{\Theta_{Gi}}$ It follows that the control input $\boldsymbol{u}$ by equation (35) is bounded. The function $\zeta_i(\mathbf{e}, \tilde{\Theta}_{Gi}, \Phi_{Gi})$ is continuous but not differentiable at the boundary between (i) and (iii). However, it is still *uniformly continuous* at this boundary because it is Lipschitz continuous at the boundary [32]. So one can apply again Barbalat's lemma to show that $\dot{V} \to 0$ as $t \to \infty$. Since $\zeta(\mathbf{e}, \tilde{\Theta}_G, \Phi_G) \le 0$ and $-\frac{1}{2}\,\mathbf{e}^{\mathrm{T}} R\mathbf{e} \le 0$, it follows that $\mathbf{e} \to 0$